Journal of Alloys and Compounds, 191 (1993) 233–238
JALCOM 496

Modulation of spin reorientation transitions in the series $R(Fe, M)_{12}X_y$ ($R \equiv Y$, Nd, Ho; $M \equiv Mo$, Ti; $X \equiv N$, H)

E. Tomey*, O. Isnard**, A Fagan***, C. Desmoulins, S. Miraglia, J. L. Soubeyroux and D. Fruchart

Laboratoire de Cristallographie du CNRS, associé à l'Université Joseph Fourier, BP 166, 38042 Grenoble Cedex 09 (France)

(Received August 17, 1992)

Abstract

The magnetic and structural properties of some $R(Fe, M)_{12}X_y$ compounds ($R \equiv Y$, Nd, $M \equiv Mo$, $X \equiv N$ and $R \equiv Ho$, $M \equiv Ti$ and $X \equiv H$) were studied by a.c. susceptibility and neutron powder diffraction. Remarkable effects can be obtained with N, H, interstitial insertion. Because of the weak magnitude of the A_{20} crystalline electric field parameter, it appears possible to modulate the anisotropic properties by N, H insertion ($y < 1$ for N, $y < 1.2$ for H). In particular, the spin reorientation transition (SRT) in $NdFe_{10.2}Mo_{1.8}$ is fixed by the introduction of N ($y \approx 0.8$). Conversely, for the system $HoFe_{11}TiH_x$ the SRT is induced by H insertion. Explanation of this phenomenon is proposed from electronic consideration based on the interstitial position in the crystal lattice.

1. Introduction

Our interest in the research of new improved hard magnetic materials being used as permanent magnets has led us to study iron-rich, rare earth (R) intermetallic compounds. A high energy density can be obtained from high saturation magnetization (Fe sublattice) and high (uniaxial) anisotropy which is the origin of the intrinsic coercivity (R sublattice).

Since 1987 [1, 2], much effort has been devoted to the $ThMn_{12}$ isotype compounds. The pure iron compound does not exist and the structure is stabilized by the introduction of a poorer valence electron metal element ($M' \equiv Al$, Cr, Mo, Re, Si, Ti, V, W). This series can be viewed as being potential magnetic materials owing to their highly desired intrinsic properties which are enhanced by interstitial insertion.

From a fundamental point of view, these systems are among the best to study the crystalline electric field (CEF) and the exchange interactions, because of the existence of only one R crystallographic site, thus eliminating all possible competition between different R sites. Also, the weak magnitude of the second-order CEF constant A_{20} makes this series an outstanding reference for the modulation of the magnetocrystalline anisotropy by interstitial insertion and Co and R substitutions.

In this paper, we have studied the effect of the interstitial elements H and N on the spin reorientation transitions (SRTs) by means of neutron powder diffraction and a.c. susceptibility ($\chi_{ac} = \chi' - j\chi''$) experiments performed between 4.2 K and room temperature.

2. Experimental procedure

The synthesis of the samples was carried out using an induction furnace and the so-called cold crucible technique. The samples were melted and levitated under a very pure Ar atmosphere (5N5). Owing to the relatively high melting point of Mo the compound was prepared in two steps. First, from stoichiometric amounts of transition metal constituent elements (purity better than 99.9%) an intermediate d metal alloy was synthesized. Secondly, after the introduction of R elements of the same purity, the final ingots were inverted and melted several times to ensure homogeneity. After cooling, the samples were wrapped in Ta foils and annealed in an atmosphere of Ar in sealed silica tubes at 950 °C for two weeks and quenched in water.

The sample homogeneity was checked by conventional X-ray powder diffraction (Cu Kα radiation). The results show that small amounts of α-Fe ($< 5\%$) are still present in the samples.

*Also at Instituto de Ciencia de Materiales de Aragon, CSIC-Universidad de Zaragoza, 50009 Zaragoza, Spain.

**Also at Institut Laue Langevin, BP 156, 38042 Grenoble Cedex 09, France.

***Also at Department of Pure and Applied Physics, Trinity College, Dublin 2, Ireland.

0925-8388/93/$6.00

The N, H insertion was carried out using dedicated stainless steel autoclaves, a moderate pressure gas (typically 1 MPa) and applying well-defined thermal cycles to the finely milled alloys (less than 50 μm). For H insertion, the sample was activated several times up to 220–250 °C, then exposed to an H_2 atmosphere until reaching a saturation state controlled with manometers. The nitrides were synthesized by reacting N_2 gas during several hours at 350 °C, the applied pressure (1 MPa) being maintained at a constant level. The amount of charged interstitial element was measured by a gravimetric method, all the samples being controlled by X-ray powder diffraction for their crystallinity and for the existence of possible extra phases, which were essentially the same as in the host compounds.

Neutron powder diffraction was performed at the Siloe Reactor of the Nuclear Centre of Grenoble (CENG) at two temperatures (4.2 K and room temperature). The refinement of the structures (nuclear and magnetic) was realized with the Rietveld method using the FULLPROF program [3]. The refinement strategy was as follows. In the first step, the overall scale factor and cell parameters for the phases were optimized; in the second step, the position parameters, occupation number, magnetic moments and isotropic temperature factors were finally refined.

The a.c. susceptibility measurements were carried out in the range from 4.2 K to room temperature using an exciting field of 1 Oe at a frequency of 120 Hz using a computer-controlled device [4].

3. Results and discussion

All the samples were found to be isotypes to $ThMn_{12}$ [5] (SG *I4/mmm*). The Mo atom was placed in the 8i position in agreement with ref. 6. The increases in cell volumes from host alloys to nitrides were 2.3% and 2.5% for the Y and Nd compounds respectively. This increase in the lattice parameters is highly anisotropic (mainly in the basal plane). The position of the N atom was found to correspond to the 2b site of the tetragonal space group, that gives rise to noticeable displacements of the 8j metal positions. The increases in T_c and cell volume are in good agreement with the values reported in ref. 7. The shortest metal–metal distances (between the 8f sites) remain almost unchanged after N insertion and can be derived directly from cell parameters ($d=c/2$).

From neutron diffraction results (Fig. 1), all the phases were found to be ferromagnets. From the magnetic intensity analysis, an SRT occurs in the $NdFe_{10.2}Mo_{1.8}$ phase. The best reliability factors are obtained with the moments along the c axis at 290 K but an X-ray pattern for an oriented powder reveals a non-strictly c axis ferromagnetic state. At present, we suggest that the fully c axis structure is only recovered at a higher temperature. Otherwise, the magnetic contributions are found more in agreement with a basal (or cone) structure at 4 K. This SRT disappears in the nitrided compound. The crystallographic and magnetic data are reported in Tables 1–4.

To check the SRT occurrence of the SRT, a.c. susceptibility measurements were performed on all the samples (Fig. 2). As the nitrogenation was carried out on finely divided and size-controlled powders, all the samples would possess the same grain size and shape to give approximately the same contribution to the demagnetizing factor which is found in the measurements (parallelism of the curves). The Nd alloy shows an SRT at 180 K, in agreement with ref. 8, but this should be a plane- (or cone-) to-cone transformation. Moreover, this reference reports that unidentified wide peaks appear for Y, Ho, Er, Tm and Lu compounds. Here, no such peaks were found in the Y compound, which suggests the possibility of relaxation extrinsic phenomena in the referenced samples as a result of spurious precipitates rather than the occurrence of a magnetic transition in the metal sublattice [9].

The a.c. susceptibility measurements performed on the $HoFe_{11}TiH_x$ suggest that the host compound shows the ferrimagnetic character of the heavy R series. However, for $x \approx 1.17$, a sharp peak was induced (Fig. 3). From ref. 10, the positions of the H atoms are distributed on two sites (16l and 32o); this fact enhances a tetrahedral site occupation neighbourhood (average planar distribution) of the R atoms, which is also shown in ref. 11. Correspondingly, Zhang and Wallace found an increase in the anisotropy field of 140–170 kOe for $SmFe_{11}TiH_x$ ($x=0$ and 1.2 respectively). In contrast, the nitrides show an enhancement of the octahedral site occupation neighbourhood (because of the occupation of one position between the two R atoms along the c axis) in opposition to the 2:17 type structures in which the N position is found in the basal plane of the hexagonal (rhombohedral) structure [12].

Analysis of these facts can be developed as follows: on the basis of the Coehoorn model [13], the second-order CEF constant can be written as

$$A_{20}=A_{20}(\mathrm{val})+A_{20}(\mathrm{lat})$$

For the lattice term, the N insertion clearly gives rise to an enhancement of the axial coordination in the R atoms while H shows a clear enhancement of the planar coordination. Recently, Li and Cadogan [14] have proposed a point-charge-based model (BCM) which takes into account the experimental data for the Nd–Fe–Ti compound; the same calculation should apply in our case. For the hydrides, the model is worse to apply,

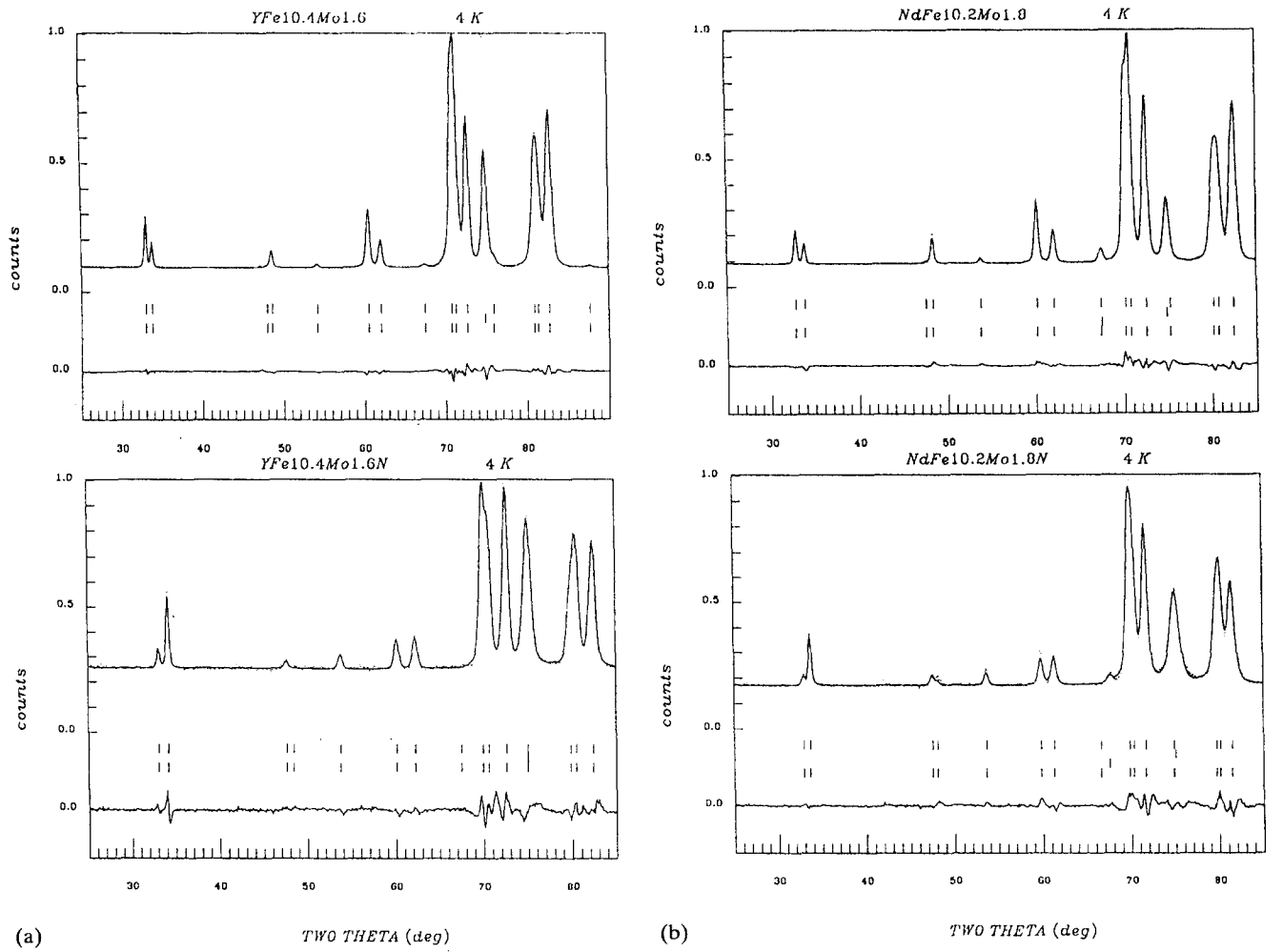

Fig. 1. Powder diffraction patterns of (a) $YFe_{10.4}Mo_{1.6}N_y$ ($y=0$, 0.9) and (b) $NdFe_{10.2}Mo_{1.8}N_y$ ($y=0$, 0.8) compounds at 4.2 K.

TABLE 1. Cell parameter values

Compound	Parameter	$x=0$		$x=0.8$		$x=0.9$	
		4.2 K	295 K	4.2 K	295 K	4.3 K	295 K
$YFe_{10.6}Mo_{1.4}N_x$	a (Å)	8.5336(4)	8.5343(4)			8.6590(8)	8.6648(6)
	c (Å)	4.7820(3)	4.7867(2)			4.7930(5)	4.8012(5)
	V (Å^3)	348.23	348.63			359.37	360.47
$NdFe_{10.2}Mo_{1.8}N_x$	a (Å)	8.5941(4)	8.5952(4)	8.6398(9)	8.646(1)		
	c (Å)	4.7816(2)	4.7908(2)	4.8437(6)	4.8519(6)		
	V (Å^3)	353.16	353.93	361.56	362.69		

because of the relatively smaller electronegativity difference between the R and the hydrogen atoms. In any case, the metal(R)–interstitial bonding is not completely understood [15] and we think that a band model accounts better for the phenomenological results than a pseudoionic model. However, the valence crystal field term is modified as follows: as a result of an increase in the electronic cloud density between the interstitial and the R atoms, the L–S coupling gives rise to changes in the ellipsoidal charge distribution of the R element, favouring the c axis easy magnetic direction (R with $\alpha_J < 0$, oblate ellipsoid) in the nitrides and the planar orientation for the hydrides. From the fact that these R-containing compounds exhibit a weakly negative A_{20} term [16], the effects on the SRTs are remarkably strong. The two parts of the second-order CEF terms shift in the same direction and enhance the axial electronic cloud for the nitrides (changing the sign of

TABLE 2. Crystal and magnetic parameters of refinements

Compound	Atom	$T=4$ K, $\lambda=2.502$ Å								$T=295$ K, $\lambda=2.502$ Å							
		Pos	x	y	z	occ.	Mx	My	Mz	Pos	x	y	z	occ.	Mx	My	Mz
$YFe_{10.4}Mo_{1.6}$	Y	2(a)	0	0	0.	1	0	0	0	2(a)	0	0	0	1	0	0	0
	Fe	8(f)	0.25	0.25	0.25	1	0	0	1.75(4)	8(f)	0.25	0.25	0.25	1	0	0	1.32(5)
	Fe	8(i)	0.3590(3)	0	0	0.56(1)	0	0	1.9(1)	8(i)	0.3593(3)	0	0	0.57(1)	0	0	1.6(2)
	Mo	8(i)				0.44(1)	0	0	0	8(i)				0.43(1)	0	0	0
	Fe	8(j)	0.2775(3)	0.5	0	1	0	0	2.3(2)	8(j)	0.2787(3)	0.5	0	1	0	0	1.4(1)
		Rp = 4.67, Rwp = 4.33, R_B = 1.21, Rm = 1.52								Rp = 4.89, Rwp = 4.44, R_B = 1.28, Rm = 1.26							
$YFe_{10.4}Mo_{1.6}N_{0.9}$	Y	2(a)	0	0	0	1	0	0	0	2(a)	0	0	0	1	0	0	0
	N	2(b)	0	0	0.5	0.8(1)	0	0	0	2(b)	0	0	0.5	0.8(1)	0	0	0
	Fe	8(f)	0.25	0.25	0.25	1	0	0	1.4(1)	8(f)	0.25	0.25	0.25	1	0	0	1.1(1)
	Fe	8(i)	0.362(1)	0	0	0.53(4)	0	0	2.2(3)	8(i)	0.362(1)	0	0	0.53(4)	0	0	1.6(3)
	Mo	8(i)				0.47(4)	0	0	0	8(i)				0.47(4)	0	0	0
	Fe	8(j)	0.277(1)	0.5	0	1	0	0	2.2(3)	8(j)	0.275(1)	0.5	0	1	0	0	1.9
		Rp = 9.82, Rwp = 8.50, R_B = 1.70, Rm = 3.80								Rp = 10.3, Rwp = 8.70, R_B = 2.22, Rm = 4.36							
$NdFe_{10.2}Mo_{1.8}$	Nd	2(a)	0	0	0	1	1.5(1)	–	2.1(1)	2(a)	0	0	0	1	0.6(3)	–	1.9(2)
	Fe	8(f)	0.25	0.25	0.25	1	1.0(1)	–	1.4(2)	8(f)	0.25	0.25	0.25	1	0.4(2)	–	1.4(1)
	Fe	8(i)	0.3607(3)	0	0	0.60(1)	1.3(1)	–	1.7(2)	8(i)	0.3604(2)	0	0	0.60(1)	0.5(2)	–	1.8(1)
	Mo	8(i)				0.40(1)	0	–	0	8(i)				0.40(1)	0	–	0
	Fe	8(j)	0.2745(3)	0.5	0	1	1.0(1)	–	1.4(2)	8(j)	0.2747(2)	0.5	0	1	0.5(2)	–	1.6(1)
		Rp = 5.47, Rwp = 4.91, R_B = 2.21, Rm = 2.58								Rp = 5.35, Rwp = 4.82, R_B = 1.36, Rm = 1.56							
$NdFe_{10.2}Mo_{1.8}N_{0.8}$	Nd	2(a)	0	0	0	1	0	0	3.5(2)	2(a)	0	0	0	1	0	0	2.7(2)
	N	2(b)	0	0	0.5	0.8(2)	0	0	0	2(b)	0	0	0.5	0.8(2)	0	0	0
	Fe	8(f)	0.25	0.25	0.25	1	0	0	2.2(2)	8(f)	0.25	0.25	0.25	1	0	0	1.9(2)
	Fe	8(i)	0.3622(9)	0	0	0.63(3)	0	0	2.3(2)	8(i)	0.3628(9)	0	0	0.62(3)	0	0	2.0(3)
	Mo	8(i)				0.37(3)	0	0	0	8(i)				0.38(3)	0	0	0
	Fe	8(j)	0.2786(8)	0.5	0	1	0	0	2.1(2)	8(j)	0.2766(9)	0.5	0	1	0	0	1.7(3)
		Rp = 9.78, Rwp = 8.53, R_B = 2.11, Rm = 2.96								Rp = 10.1, Rwp = 8.61, R_B = 2.09, Rm = 2.21							

TABLE 3. Shortest metal–metal distances less than 3 Å (from neutron powder diffraction at 295 K)

	Atom number	$YFe_{10.6}Mo_{1.4}N_x$		$NdFe_{10.2}Mo_{1.8}N_x$	
		$x=0$	$x=0.9$	$x=0$	$x=0.8$
Fe(8i), Fe(8i), (Mo)	1	2.402(4)	2.39(1)	2.400(2)	2.37(1)
	4	2.935(1)	2.935(5)	2.935(1)	2.949(4)
Fe(8j)	2	2.664(1)	2.664(7)	2.649(1)	2.669(5)
	2	2.667(2)	2.678(6)	2.661(1)	2.709(5)
Fe(8f)	4	2.618(1)	2.660(3)	2.6367(6)	2.664(3)
Fe(8j), Fe(8j)	2	2.671(3)	2.76(1)	2.737(2)	2.732(8)
Fe(8f)	4	2.4585(3)	2.486(1)	2.4693(2)	2.489(1)
Fe(8f), Fe(8f)	2	2.3933(1)	2.4006(3)	2.3954(1)	2.4260(3)

TABLE 4. Shortest metal-metal distances less than 3 Å (from neutron powder diffraction at 4.2 K)

	Atom number	$YFe_{10.6}Mo_{1.4}N_x$		$NdFe_{10.2}Mo_{1.8}N_x$	
		$x=0$	$x=0.9$	$x=0$	$x=0.8$
Fe(8i), Fe(8i), (Mo)	1	2.406(3)	2.39(1)	2.394(4)	2.38(1)
	4	2.935(1)	2.934(6)	2.929(2)	2.949(4)
Fe(8j)	2	2.656(1)	2.683(8)	2.640(2)	2.685(5)
	2	2.659(1)	2.685(8)	2.656(2)	2.712(5)
Fe(8f)	4	2.616(1)	2.656(4)	2.656(2)	2.659(3)
				2.636(1)	
Fe(8j), Fe(8j)	2	2.685(3)	2.72(1)	2.749(3)	2.705(7)
Fe(8f)	4	2.457(1)	2.485(1)	2.4672(2)	2.488(1)
Fe(8f), Fe(8f)	2	2.3910(1)	2.3965(2)	2.3908(1)	2.4219(3)

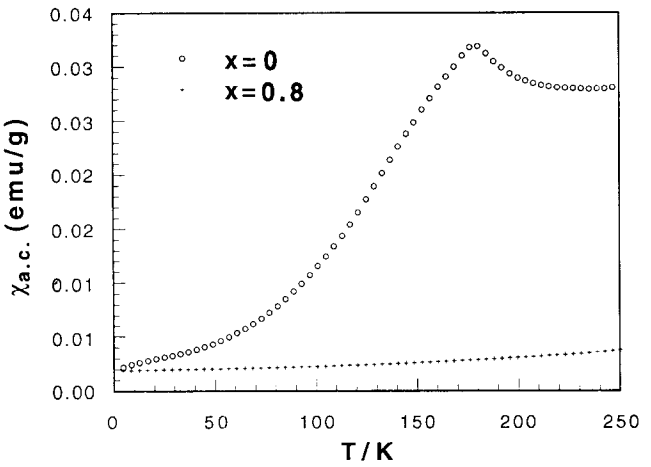

Fig. 2. Curves of a.c. susceptibility for $NdFe_{10.2}Mo_{1.8}N_y$ ($y=0$, 0.8).

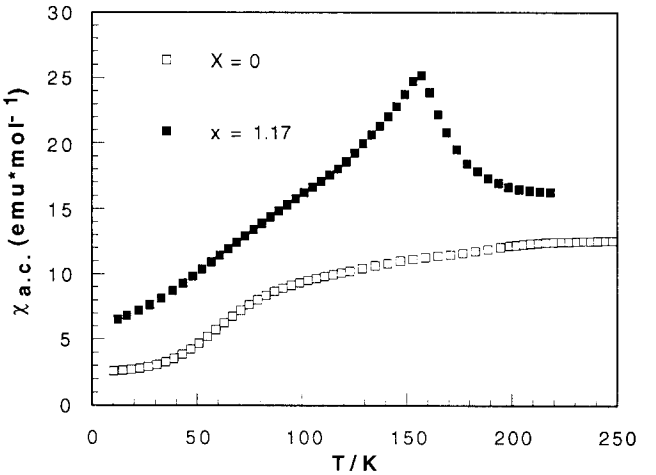

Fig. 3. Curves of a.c. susceptibility for $HoFe_{11}TiH_y$ ($y=0$, 1.17).

A_{20} [14, 17]) and the planar orientation (increase of this value) for the hydrides, according to the experimental results.

4. Conclusions

The $RFe_{12-x}M_x$ series of alloys with the $ThMn_{12}$-type structure exhibits two interesting phenomena. They show good potential permanent magnet properties for compounds with low rare earth concentrations. They are also good references to test the CEF scheme and the exchange interaction forces since there is only one R site. It is easy to modulate anisotropy using N and H interstitial insertion. This has been found previously to perturb the CEF parameters. This fundamental

approach can assist the development of new synthesis routes for hard magnetic materials.

Acknowledgments

This work was performed under Brite-Euram Contract BE 4393-90 which two of us (ET and AF) received. Thanks are due to the Département de Recherches Fondamentales du Centre d'Etudes Nucléaires de Grenoble for providing us with neutron scattering facilities.

References

1 K. Ohashi, T. Yokohama, R. Osugi and Y. Tawara, *IEEE Trans. Magn., 23* (5) (1987).
2 D. B. de Mooij and K. H. J. Buschow, *Philips J. Res., 42* (1987) 246.
3 J. Rodriguez-Carvajal, *XVth Cong. Int. Union of Crystallogr.*, Satellite Meeting on Powder Diffraction, Toulouse, 1990, p. 127.
4 C. Rillo, F. Lera, A. Badía, L. Angurel, J. Bartolomé, F. Palacio, R. Navarro and A. J. Van Duyneveldt, in R. A. Hein, J. L. Francavilla and D. H. Liebenberg (eds.), *Magnetic Susceptibility of Superconductors and other Spin Systems,* Plenum, NY, 1992.
5 J. V. Florio, R. E. Rundle and A. I. Snow, *Acta Crystall., 5* (1951) 449.
6 K. H. J. Buschow, in I. V. Mitchell (ed.), *CEAM Rep.,* 1989.
7 M. Anagnostou, C. Christides and D. Niarchos, *Solid State Commun., 78* (8) (1991) 681.
8 X. C. Kou, C. Christides, R. Grössinger, H. R. Kirchmayr and A. Kostikas, *J. Magn. Magn. Mater, 104–107* (1992) 1341.
9 F. J. Lázaro, L. M. García, J. Bartolomé, D. Fruchart and S. Miraglia, *Proc. ICM'91, J. Magn. Magn. Mater., 114* (1992) 261.
10 S. Obbade, S. Miraglia, D. Fruchart, M. Pre, P. L'Heritier and A. Barlet, *CR Acad. Sci. Paris, Sér. II 307* (1988) 889.
11 L. Y Zhang and W. E. Wallace, *J. Alloys Comp., 149* (1989) 371.
12 J. M. D. Coey, H. Sun, D. P. F. Hurley, *J. Magn. Magn. Mater., 101* (1991) 310.
13 R. Coehoorn, *J. Magn. Magn. Mater., 99* (1991) 55.
14 H. S. Li and J. M. Cadogan, *J. Magn. Magn. Mater., 109* (1992) L153.
15 L. E. Toth, *Refractory Materials,* Vol. 7, *Transition Metal Carbides and Nitrides,* Academic Press, New York, 1971, Ch. 8.
16 B. P. Hu, H. S. Li, J. P. Gavigan and J. M. D. Coey, *J. Phys., 1* (1989) 755.
17 Y. C. Yang, Y. D. Zhang, L. S. Kong, Q. Pan and S. L. Ge, *Solid State Commun., 78* (4) (1991) 317.